

Fluorescent II-VI Semiconductor Quantum Dots: Potential Tools for Biolabeling and Diagnostic

Patrícia M. A. Farias,^{*a} Adriana Fontes,^a André Galembeck,^b Regina C. B. Q. Figueiredo^c
and Beate S. Santos^d

^aDept. de Biofísica e Radiobiologia, CCB, ^bDept. de Química Fundamental, CCEN

^dDept. de Ciências Farmacêuticas, CCS, Universidade Federal de Pernambuco, 50670-901 Recife-PE, Brazil

^cCentro de Pesquisas Aggeu Magalhães, Dept. de Biologia Celular e Ultraestrutura, FIOCRUZ,
50670-902 Recife-PE, Brazil

No presente artigo são apresentados e discutidos, resultados obtidos pelo uso de quantum dots de semicondutores altamente luminescentes, obtidos por métodos de síntese coloidal. Os quantum dots apresentam superfície hidrofílica e pH fisiológico. Foram sintetizados em meio aquoso e funcionalizados com compostos orgânicos para utilização em diagnóstico preciso de câncer de mama (carcinoma ductal infiltrante), câncer de cérebro (glioblastoma) e câncer cervical (colo de útero).

In this work we show and discuss the results obtained by using highly luminescent colloidal hydrophilic semiconductor Quantum Dots, synthesized in aqueous medium, physiological pH and functionalized with organic compounds for precise diagnostic of breast (ductal filling carcinoma), brain (glioblastoma) and cervical cancer.

Keywords: semiconductor nanoparticles, quantum dots, biolabeling, diagnostics

Introduction

Fluorescence provides an important tool for the investigation of basic physical and chemical properties of biological structures. The high sensitivity of fluorescence, combined with the advances in measurement techniques, permits detection of ultra small quantities of specific species present in biological systems. There is a large variety of compounds which are commonly used as fluorescent dyes for biolabeling, such as: organic molecules, fluorescent proteins, metal chelators, chemi- and bioluminescent agents. All of these dyes present one or more of the following disadvantages: lack of brightness, narrow excitation bands and high photobleaching rate (see Figure 1). In the last decade a new class of fluorescent materials known as quantum dots (QDs) has been tested as biolabels. Quantum dots are nanometric inorganic crystals, which present special characteristics due to the fact that they are in quantum confinement regimen.¹⁻³ In the case of semiconductor quantum dots, one of these

special characteristics is the capability of tuning their optical properties, particularly their emission spectra⁴ by controlling the size of the particles. In spite of the fact that quantum dots have been used for distinct applications since the 70's, their first application as biomarkers was simultaneously reported in 1998^{5,6} by Bruchez *et al.*⁵ and Chan *at al.*⁶ In these works, CdSe QDs coated with silica and mercaptoacetic acid layers, respectively, were synthesized and used by both groups to specific biolabeling of living cells, by covalent coupling of ligands to cell surface receptors. Subsequently, several authors have reported labeling of cells and of tissue sections using several different surface modifications of QDs.⁷⁻¹¹

The attachment of biomolecules to nanometer-sized bits of semiconductors, results in a sensitive and potentially widely applicable method for detecting biomolecules and for scrutinizing biomolecular processes.¹²⁻¹³ The quantum dot-labeled molecules remain active for biochemical reactions and the tagged species produce brightly colored products.^{5,6} This methodology takes advantage of the efficient fluorescence and high photostability of the semiconductor dots, representing a new class of biological stains.

*e-mail: pmaf@ufpe.br

In the pursuit of sensitive and quantitative methods to detect and diagnose cancer, nanotechnology has been identified as a field of great promise. Quantum dots application in the investigation of neoplastic processes, as well as, in the development of new protocols for cancer diagnostics, take into account, specific features concerning quantum confinement of the dots, as well as, features related to changes in the physical properties and metabolic regimen of neoplastic cells.

Hydrophilic quantum dots in water medium and at physiological pH conditions have the potential to expand conventional protocols used for cancer diagnostic, which need previous tissue/cell fixation, and extend it to investigate living cellular and tissular neoplastic mechanisms in real time. In this work, we show and discuss the results obtained by conjugating CdS/Cd(OH)₂ highly fluorescent quantum dots with living healthy and neoplastic breast, glial and cervical tissues and cells.

Methodology

The core-shell luminescent CdS/Cd(OH)₂ QDs were obtained by reacting Cd²⁺ and S²⁻ in aqueous solution in the presence of sodium polyphosphate (Sigma-Aldrich) as the stabilizing agent. Subsequent surface passivation with Cd(OH)₂ was carried out to improve luminescence. At a pH of 7.2 the QDs were functionalized with a 0.01% glutaraldehyde solution (QD-glut), as described in a previous work.¹⁴ The glutaraldehyde is a bi-dentate homofunctional organic functionalizing agent. In this case, glutaraldehyde molecules attached to QDs surface, intermediate the interaction of the QDs with the living healthy and neoplastic cells. Cervical cells and breast cancer samples were labeled in saline solution (NaCl 0.9%) while the glial (healthy and neoplastic ones) were labeled directly in their culture media. The labeling process (also named incubation) was performed at room temperature (25 °C). Tissue and cell staining were evaluated by the laser scanning confocal microscopy, by using Leica TCS SP2 AOBS (breast and cervical cells/tissues) and LSM 510 Carl Zeiss (for glial and glioblastoms cells) confocal microscopes. The acquisition parameters were maintained constant for all the analyzed samples, in order to compare the labeling efficiency in the distinct biological samples investigated. The images were further processed using the software Leica Lite and LSM 510 (Carl Zeiss Inc.). Laser Scanning Confocal Microscopy measurements were also performed at room temperature and at different time intervals in order to monitor the time evolution of the interaction between the QDs and the cells or tissues. Fluorescence Microscopy (Carl Zeiss Inc.) was used as a primary tool in order to explore the labeling of the samples.

Next section will present the results obtained by Laser Scanning Confocal Microscopy using an apochromatic water immersion, 63× with numerical aperture of 1.2 objective lens. Two wavelengths were used to promote excitation of the marked samples: 488 and 543 nm. The recorded image in each case was taken using dual-channel scanning and consisted of 1024×1024 pixels. For each cell type the images were reproduced at least three times, and to establish a comparative analysis of the luminescence intensity maps the parameters related to the acquisition of confocal images, such as pinhole, filters, beam splitters and photomultiplier gain and off-set were maintained constant.

Results and Discussion

Structural characterization of the QDs was performed by X-ray Diffraction and by Electronic Transmission Microscopy experiments. A representative Transmission Electronic Microscopy image of the core-shell CdS/Cd(OH)₂ quantum dots functionalized with glutaraldehyde is shown in Figure 1, in which the scale bar corresponds to 40 nanometers (nm). The averaged size of the QDs is about 9 nm. Optical characterization of the QDs was done by spectroscopic techniques. Figure 2 illustrates the excitation and emission spectra for as prepared core-shell CdS/Cd(OH)₂ quantum dots, in which may be observed a broad excitation band and a narrow gaussian emission band of about 50 nm (FWHM).

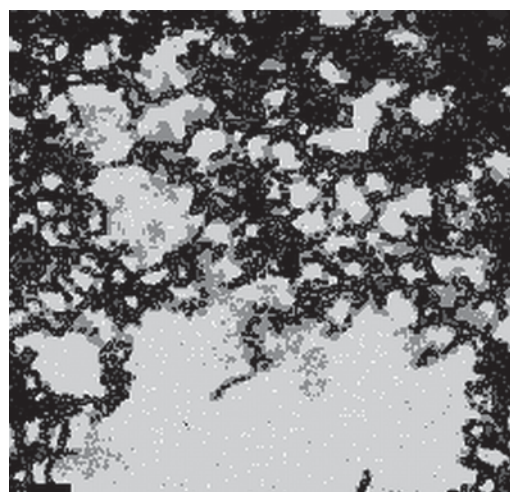


Figure 1. Transmission Electronic Microscopy image of the CdS/Cd(OH)₂ core shell quantum dots. Scale bar: 40 nm.

Figures 3 and 4 show confocal microscopy images (left) and corresponding fluorescence intensity maps (right) for the healthy and neoplastic glial cells and the corresponding incubation time of the cells with the functionalized QDs-

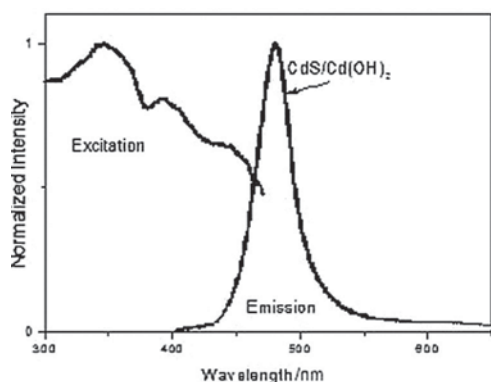


Figure 2. Excitation and emission spectra of as prepared CdS/Cd(OH)₂ quantum dots.

glut. At the fluorescence intensity maps, the dark grey regions correspond to the absence of fluorescence, while the light grey regions correspond to regions of highest fluorescence intensities.

Figure 5 shows Transmission Electronic Microscopy image of glioblastoma labeled cell, in which the highest QDs concentration is nearby the nuclear envoltorium.

Breast cancer tissues samples were incubated with the functionalized QDs-glut, and as can be noticed at Figure 6, the neoplastic cells filling up the mammary duct clearly

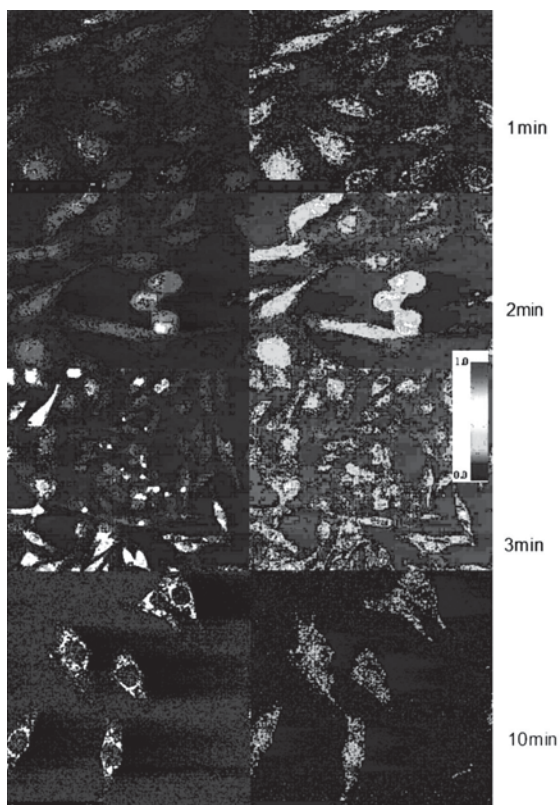


Figure 3. Neoplastic glial (glioblastoma) cells incubated with QDs-Glut. Left: Confocal Microscopy image. Right: corresponding fluorescence intensity maps. (min = minute(s))

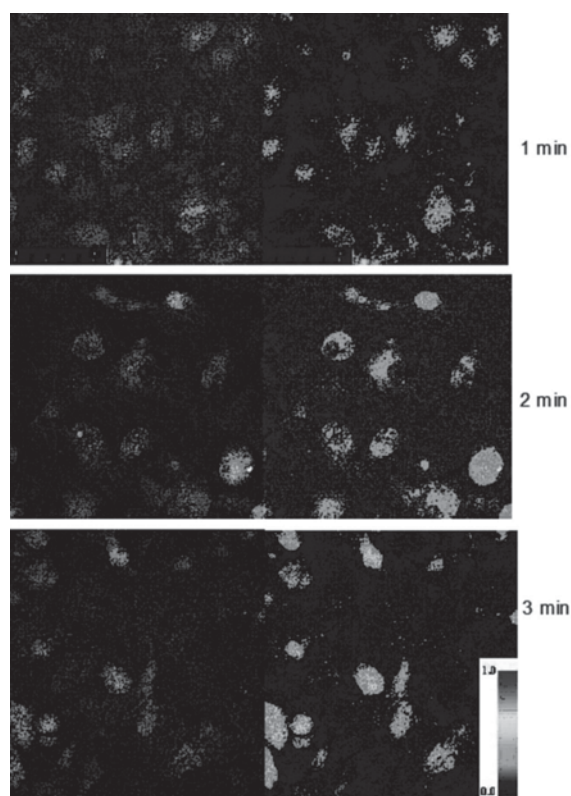


Figure 4. Healthy glial cells incubated with QDs-Glut. Left: Confocal Microscopy image. Right: corresponding fluorescence intensity maps. (min = minute(s)).

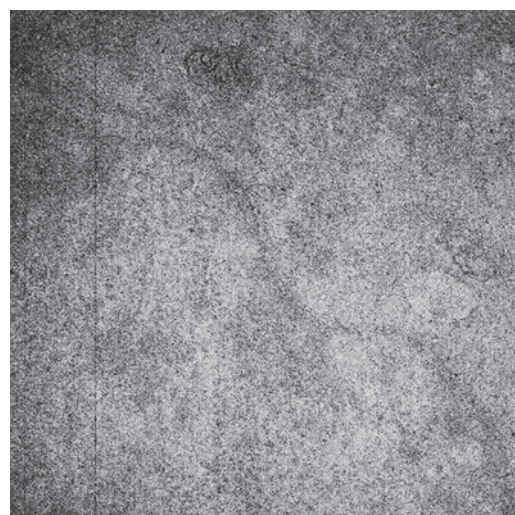


Figure 5. Transmission Electronic Micrography image of Glioblastoma labeled cells: highest QDs concentration at the nuclear envoltorium.

show highest QDs concentrations than the normal cells of the same sample.

Figure 7 shows confocal microscopy image and fluorescence intensity maps for QDs labeled cervical intra-epithelial neoplastic cells 3 (INC3), while Figure 8 show confocal microscopy image, fluorescence intensity map and transmission microscopy overlapped with

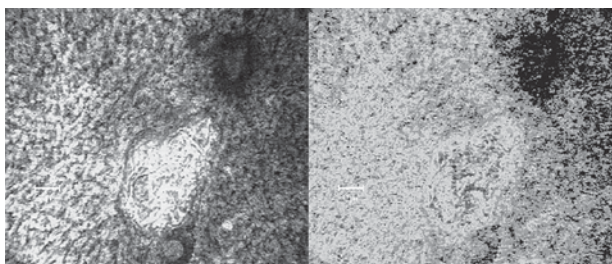


Figure 6. Left: Confocal Microscopy image of filling ductal carcinoma. Right: Corresponding fluorescence intensity map.

fluorescence image of cervical cells presenting severe dyskaryosis, which is the last stage prior to cervical cancer. The images shown at Figures 7 and 8, represent processes which result from the infection of cervical cell by Human Papillomaviruses (HPV).

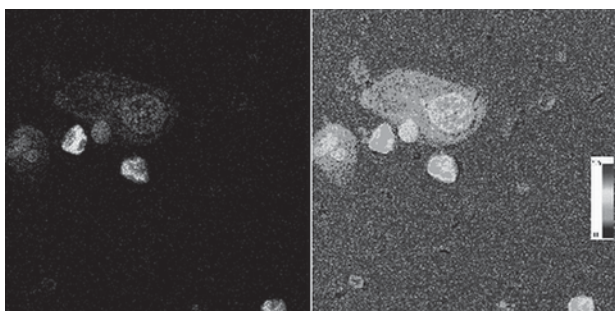


Figure 7. Cervical intra-epithelial neoplastic cells 3 (INC3). Left: Confocal microscopy image. Right: Fluorescence intensity map.

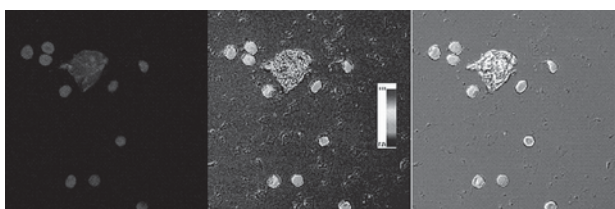


Figure 8. Confocal microscopy image (left), fluorescence intensity map (center) and transmission microscopy overlapped with fluorescence image (right) of cervical cells presenting severe dyskaryosis (last stage prior to cervical cancer).

The living cells did not show any sign of damage after the conjugation procedure with the QDs and maintained their integrity even after five days of incubation time, demonstrating the low toxicity of the QDs for *in vitro* studies. The time evolution of the interaction cells-QDs shown in Figures 3 and 4 above clearly reveals different labeling patterns as well as different fluorescence intensities. It also can be noticed that the CdS-Cd(OH)₂-Glut QDs easily interacts with both healthy and neoplastic. As mentioned above, the glutaraldehyde is a homofunctional bidentate ligand, which promotes hemi-acetal interactions

with the QDs outer shell, at the same time that binds to cell proteins by Schiff's base interactions.¹³⁻¹⁴

The observed fluorescence in quantum dots, which allows their use as efficient fluorescent biolabels, is produced upon the recombination of the charge carriers which are generated by light absorption. The first colloidal obtained nanocrystals showed a very low fluorescence quantum yield ($\phi < 1\%$). The non-radiative processes involved in semiconductor nanocrystals are described to have the same physico-chemical nature as those observed in bulk semiconductor materials. Taking into account the high number of surface atoms compared to bulk atoms, it was suggested that the main contribution for this was that the prepared colloidal particles had a lot of surface defect sites (shallow and deep traps) where radiationless recombination of the charge carriers occurred.¹

Cancer is a complex disease caused by genetic instability and accumulation of multiple molecular alterations, which are related to a wide variety of modifications in cell and tissues properties such as: (i) increasing cell membrane permeability and hydraulic conductivity, which are in general, significantly higher than in normal cells and (ii) increasing the membrane channels and pores sizes. In tumor tissues the blood vessels are leaky, also presenting larger pore sizes compared to normal tissues (28). The above mentioned features play an important role in the internalization of quantum dots by cancer cells and tissues. The results presented and discussed in the previous section, clearly indicate that most probably there are two different cell (or tissue)/QDs interaction mechanisms which compete kinetically: (i) quantum dots interaction with surface proteins, which occurs by the formation of Schiff's bases between amine terminals of these proteins and the terminal carboxyl group of the quantum dots functionalizing agent (glutaraldehyde) and (ii) quantum dot up take *via* endocytosis, which depending on the cellular molecules involved in the internalization process, may be preferable named by pinocytosis or phagocytosis. While these last processes do differ in details, their common feature is that cells engulf the material to be incorporated. In the labeling procedures described in this work, the endocytosis mechanisms were prevalent in the interaction between cancer cells (or tissues) and quantum dots. Transmission electronic results indicated that the fluid phase endocytosed CdS/Cd(OH)₂ larger quantum dots (9nm) were predominantly localized in granular compartments around the nuclear region, while the smaller ones (6 nm) We also observed that after cell division, the larger QDs can be found not only in the perinuclear region but also in cytosol regions. Beyond this, upon cell division the ingested quantum dots are distributed between both cells.¹⁵

Acknowledgements

The authors would like to thank Dr. Carlos A. P. Leite (Universidade Estadual de Campinas - UNICAMP) for the electronic micrographies, as well as, Philips Corp., CNPq, CEPOF, Fapesp, IMMC, Renami and Facepe Brazilian Agencies for the financial support.

References

1. Borchert H.; Talapin, D. V.; McGinley, C.; *J. Chem. Phys.* **2003**, *271*, 1800.
2. Alivisatos, A. P.; *Science* **1996**, *271*, 933.
3. Nowak, C.; Döllefeld, H.; Eychmüller, A.; *J. Chem. Phys.* **2001**, *114*, 489.
4. Eychmüller, A.; *J. Phys Chem. B.* **1996**, *59*, 13226.
5. Bruchez Jr, M. P.; Moronne, M.; Gin, P.; Weiss, S.; Alivisatos, A.P.; *Science* **1998**, *281*, 2013.
6. Chan, W. C. W.; Nie, S.; *Science* **1998**, *281*, 2016.
7. Ballou, B.; Lagerholm, B. C.; Ernst, L. A.; Bruchez, M. P.; Waggoner A. S.; *Bioconjugate Chem.* **2004**, *15*, 79.
8. Gao, X.; Nie, S.; *Trends Biotech.* **2003**, *21*, 371.
9. Äkerman, M. E.; Chan, W. C. W.; Laakkonen, P.; Bhatia, S. N.; Ruoslahti, E.; *Appl. Biol. Sci.* **2002**, *99*, 12617.
10. Chan, W. C. W.; Maxwell, D. J.; Gao, X.; Bailey, R. E.; Han, M.; Nie, S.; *Curr. Opin. Biotechnol.* **2002**, *13*, 40.
11. Mattheakis, L. C.; Dias, J. M.; Choi, Y.; Gong, J.; Bruchez, M. P.; Liu, J.; Wang, E.; *Anal. Biochem.* **2004**, *327*, 200.
12. Petrov, D. V.; Santos, B. S.; Pereira, G. A. L.; Donegá, C. M.; *J. Phys. Chem. B.* **2002**, *106*, 5325.
13. Farias, P. M. A.; Santos B. S.; Menezes, F. D.; Ferreira, R. C.; Barjas-Castro, M. L.; Castro, V.; Lima P. R. M.; Fontes A.; Cesar, C. L.; *J. Microsc.* **2005**, *219*, 103.
14. Farias, P. M. A.; Santos, B. S.; Menezes, F. D.; Ferreira, R. C.; Barjas-Castro, M. L.; Castro, V.; Lima, P. R. M.; Fontes A.; Cesar, C. L.; *J. Biomed. Opt.* **2005**, *10*, 44023.
15. Farias, P. M. A.; Santos, B. S.; Menezes, F. D.; Ferreira, R.; Fontes, A.; Carvalho, H. F.; Romão, L.; Moura-Neto V.; Amaral, J. C. O. F.; Cesar, C. L.; Figueiredo, R. C. B. Q.; Lorenzato, F. R. B.; *Phys. Status Solidi C.* **2006**, *11*, 4001.

Received: July 23, 2007

Published on the web: February 22, 2008

FAPESP helped in meeting the publication costs of this article.